

# Intramolecular Rearrangements in Six-Coordinate Ruthenium and Iron Dihydrides

Chirine Soubra,<sup>†</sup> Yasuo Oishi,<sup>‡</sup> Thomas A. Albright,<sup>\*,†</sup> and Hiroshi Fujimoto<sup>‡</sup>

Department of Chemistry, University of Houston, Houston, Texas 77204-5641, and  
Division of Molecular Engineering, Kyoto University, Kyoto 606, Japan

Received June 6, 2000

Molecular orbital calculations at the ab initio level are used to study polytopal rearrangements in  $\text{H}_2\text{Ru}(\text{PH}_3)_4$  and  $\text{H}_2\text{Fe}(\text{CO})_4$  as models of 18-electron, octahedral metal dihydrides. It is found that, in both cases, the transition state for these rearrangements is a dihydrogen species. For  $\text{H}_2\text{Fe}(\text{CO})_4$ , this is a square pyramidal complex where the  $\text{H}_2$  ligand occupies an apical position and is rotated by  $45^\circ$  from its original orientation. This is precisely analogous to the transition state for Fe–olefin rotation in (olefin)Fe(CO)<sub>4</sub> complexes and has a very similar electronic origin. Another transition state very close in energy is found wherein the basic coordination geometry is a trigonal bipyramid and the  $\text{H}_2$  ligand is coordinated in the axial position. For  $\text{H}_2\text{Ru}(\text{PH}_3)_4$ , the former stationary point lies at a much higher energy and the latter clearly serves as the transition state for hydride exchange. The reason for this difference is discussed along with the roles of electron correlation in the two compounds.

## Introduction

Stereochemical nonrigidity in six-coordinate molecules has attracted considerable interest among researchers because six-coordinate molecules were thought to be rigid, with the predominant coordination polyhedron being the octahedron. In contrast, nonrigidity in five-, seven-, eight-, and nine-coordinate molecules is a common feature and is thought to be a reflection that there is no dominance of an idealized coordination polyhedron in these coordination classes.<sup>1–5</sup> Several research groups, however, have reported nonrigidity<sup>6–11</sup> in six-coordinate metal carbonyl and phosphine derivatives. On the other hand, a group of transition metal hydrides of the type  $\text{H}_2\text{ML}_4$  (M = Fe or Ru; L = phosphine or phosphite) have been shown<sup>12</sup> to undergo such reactions. This special class of  $\text{H}_2\text{ML}_4$  complexes undergo rearrangements with much lower activation barriers than those found for most other octahedral complexes. Several mechanisms<sup>5,13–19</sup> have been proposed for the polytopal rear-

rangements of d<sup>6</sup> octahedral transition metal complexes. These reactions have been studied primarily by Muetterties and co-workers<sup>1,5,14,15</sup> for a class of six-coordinate transition metal hydrides of the type  $\text{H}_2\text{ML}_4$  (where L is a phosphite, phosphine, phosphinite, or phosphonite). The free energies of activation for isomerization have been determined experimentally<sup>1</sup> for some iron and ruthenium dihydrides. These fall in the range of ~12–15 kcal/mol for the iron dihydrides, whereas the ruthenium barriers were found to be somewhat larger, in the range of ~16–20 kcal/mol. We have sought to establish the rearrangement mechanism(s) for  $\text{H}_2\text{Ru}(\text{PH}_3)_4$  and  $\text{H}_2\text{Fe}(\text{CO})_4$ , two representative octahedral transition metal dihydrides, by means of ab initio molecular orbital calculations as described in the next section.

## Computational Details

All ab initio molecular orbital computations were carried out with the Gaussian 82,<sup>20</sup> Gaussian 90,<sup>21</sup> and gaussian 92<sup>22</sup> packages. Three basis sets were used for the ruthenium complexes. The first was used for geometry optimization where an ECP2 effective core potential<sup>23</sup> was used to describe the core orbitals of the metal and the valence 4s, 4p, 4d, 5s, and 5p orbitals were treated explicitly with an associated double- $\zeta$  basis. The phosphorus atom has an ECP1 effective core potential which includes 2s and 2p orbitals, and a minimal basis set depicts the 3s and 3p orbitals. The two hydrogen atoms connected to

<sup>†</sup> University of Houston.

<sup>‡</sup> Kyoto University.

- (1) Meakin, P.; Muetterties, E. L.; Jesson, J. P. *J. Am. Chem. Soc.* **1973**, *95*, 75.
- (2) Darensbourg, D. J.; Graves, A. H. *Inorg. Chem.* **1979**, *18*, 1257.
- (3) Darensbourg, D. J.; Baldwin, B. J. *J. Am. Chem. Soc.* **1979**, *101*, 6447.
- (4) Van-Catledge, F. A.; Ittel, S. D.; Jesson, J. P. *Organometallics* **1985**, *4*, 18.
- (5) Tebbe, F. N.; Meakin, P.; Jesson, J. P.; Muetterties, E. L. *J. Am. Chem. Soc.* **1970**, *92*, 1068.
- (6) Darensbourg, D. J. *Inorg. Chem.* **1979**, *18*, 14.
- (7) Darensbourg, D. J.; Kudarski, R.; Schenk, W. *Inorg. Chem.* **1982**, *21*, 2488.
- (8) Darensbourg, D. J.; Gray, R. L. *Inorg. Chem.* **1984**, *23*, 2993.
- (9) Darensbourg, D. J.; Darensbourg, M. Y.; Gray, R. L.; Simmons, D.; Arndt, L. W. *Inorg. Chem.* **1986**, *25*, 880.
- (10) Ismail, A. A.; Sauriol, F.; Butler, I. S. *Inorg. Chem.* **1989**, *28*, 1007.
- (11) Pomeroy, R. K.; Graham, W. A. G. *J. Am. Chem. Soc.* **1972**, *94*, 274.
- (12) Muetterties, E. L. *Acc. Chem. Res.* **1970**, *3*, 266.
- (13) Bailar, J. C., Jr. *J. Inorg. Nucl. Chem.* **1958**, *8*, 165.
- (14) Meakin, P.; Guggenberger, L. J.; Jesson, J. P.; Gerlach, D. H.; Tebbe, F. N.; Peet, W. G.; Muetterties, E. L. *J. Am. Chem. Soc.* **1970**, *92*, 3482.
- (15) Meakin, P.; Muetterties, E. L.; Tebbe, F. N.; Jesson, J. P. *J. Am. Chem. Soc.* **1971**, *93*, 4701.
- (16) Alex, R. F.; Pomeroy, R. K. *J. Organomet. Chem.* **1985**, *284*, 379.
- (17) Rodger, A.; Johnson, B. F. G. *Inorg. Chem.* **1988**, *27*, 3062.

- (18) Hansen, L. M.; Marynick, D. S. *Inorg. Chem.* **1990**, *29*, 2482.
- (19) Ball, G. E.; Mann, B. E. *J. Chem. Soc., Chem. Commun.* **1992**, 561. Mann, B. E. Personal communications.
- (20) Binkley, J. S.; Frisch, M.; Raghavachari, K.; Fluder, E.; Seeger, R.; Pople, J. A. *Gaussian 82*; Carnegie-Mellon Publishing Unit: Pittsburgh, PA, 1982.
- (21) Frisch, M. J.; Head-Gordon, M.; Trucks, G. W.; Foresman, J. B.; Schlegel, H. B.; Raghavachari, K.; Robb, M. A.; Binkley, J. S.; Gonzalez, C.; Defrees, D. J.; Fox, D. J.; Whiteside, R. A.; Seager, R.; Melius, C. F.; Baker, J.; Martin, R. L.; Khan, L. R.; Stewart, J. J. P.; Topiol, S.; Pople, J. A. *Gaussian 90*; Gaussian Inc.: Pittsburgh, PA, 1990.
- (22) Frisch, M. J.; Trucks, G. W.; Head-Gordon, M.; Gill, P. M. W.; Wong, M. W.; Foresman, J. B.; Johnson, B. J.; Schlegel, H. B.; Robb, M. A.; Replogle, E. S.; Gomperts, R.; Andres, J. L.; Raghavachari, K.; Binkley, J. S.; Gonzalez, C.; Martin, R. L.; Fox, D. J.; Defrees, D. J.; Baker, J.; Stewart, J. J. P.; Pople, J. A. *Gaussian 92*; Gaussian Inc.: Pittsburgh, PA, 1992.
- (23) Wadt, W. R.; Hay, P. J. *J. Chem. Phys.* **1985**, *82*, 284.

the metal were treated with a 4-31G basis,<sup>24</sup> whereas the hydrogens connected to the phosphorus atoms were treated with an STO-3G basis.<sup>25</sup> Basis I was the same as the basis set previously described except that an ECP2 core and associated double- $\zeta$  basis for phosphorus and 3-21G basis for hydrogen<sup>30</sup> were used. Basis II used triple  $\zeta$  on 4d and 5p orbitals and added 4f orbitals on ruthenium.<sup>26</sup> The ligands were treated with the same basis as in basis set I, except for the two hydrogens connected to ruthenium which were treated with a 6-311G\*\* basis.<sup>27</sup>

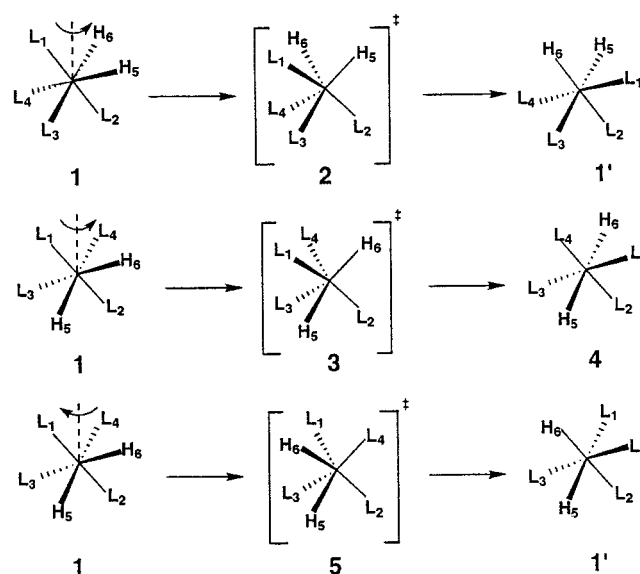
Three basis sets, III–V, were used for the iron complexes. In III, the Fe basis started from Huzinaga's (4333/43/4) primitive set.<sup>28</sup> The d along with the 4s and augmented 4p functions were replaced by functions optimized for molecular environments<sup>29</sup> to yield a basis set of the form (4333/433/31). The standard 3-21G basis<sup>30</sup> was used for C and O atoms, and the 4-31G basis was used for H. Basis IV used an ECP2 effective core potential which included 3s and 3p and double  $\zeta$  for 3d, 4s, and 4p on Fe. The 3-21G basis was employed for C and O, and the 4-31G basis was used for H. Basis V applied an ECP2 effective core potential on core orbitals up to 3p, double  $\zeta$  on 4s, and triple  $\zeta$  on 4p and 3d and added an f function on the metal. The 3-21G basis was used for C and O, while H was treated with the 6-311G\*\* basis.

All geometries were fully optimized and verified by subsequent numerical Hessian calculations. Full geometrical details along with the absolute energies are available upon request from the authors. Optimizations and frequencies were computed at the MP2 level<sup>31</sup> for the ruthenium complexes using basis I and at the Hartree–Fock (HF) level for the iron complexes using basis III. An extensive study was undertaken regarding the effects of electron correlation on the relative stabilities of the transition state structures. The correlated methods include MP4(SDQ),<sup>32</sup> where triple substitutions are not included, quadratic CI with single and double substitutions (QCISD)<sup>33</sup> and evaluation of the triple substitutions (QCISD(T)), and coupled cluster with single and double substitutions (CCSD)<sup>34</sup> and the evaluation of the contributions of single and triple excitations through fourth order using the CCD function (ST4CCD).<sup>35</sup> The **Z** matrixes and total energies for all structures may be obtained from the authors. Optimizations and frequency calculations were also performed using the density functional theory (DFT) hybrid methods: HFB, B3P86, and Becke3LYP.<sup>36–41</sup> Basis II for  $\text{H}_2\text{Ru}(\text{PH}_3)_4$  and basis IV along with basis V for  $\text{H}_2\text{Fe}(\text{CO})_4$  were utilized in the DFT calculations.

### Possible Mechanisms of Intramolecular Rearrangements

Before the results of our theoretical investigation are presented, the proposed mechanisms are enumerated for the polytopal rearrangements of  $d^6$  octahedral transition metal complexes regarding those pathways that relate to exchange in

### Scheme 1



the  $\text{H}_2\text{ML}_4$  case. The first pathway, which was proposed by Bailar in 1958,<sup>13</sup> is the trigonal twist mechanism. This process involves a rotation of three metal–ligand bonds (two M–L bonds and one M–H bond or two M–H bonds and one M–L bond) around one of the  $C_3$  axes. There are three possible, distinct ways for an  $\text{H}_2\text{ML}_4$  molecule to undergo this rearrangement. These are shown in Scheme 1. The first rearrangement pictured in the scheme involves the twist of two M–H bonds and one M–L bond which rotate counterclockwise and results in the formation of **1'** passing through a trigonal prismatic transition state structure, **2**. If we consider the same twist but rotate clockwise, we obtain exactly the same pathway. The remaining two paths involve the twist of two M–L bonds and one M–H bond. Rotating counterclockwise in the middle of Scheme 1 results in a cis–trans isomerization via transition state **3**. Other possibilities, of course, exist; these serve only to permute the carbonyl or phosphine ligands.

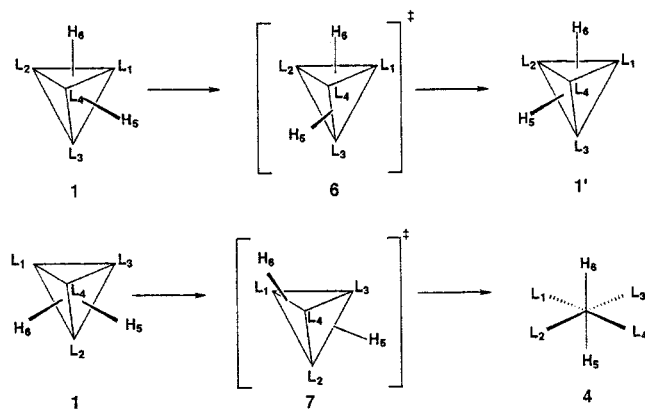
The tetrahedral jump mechanism<sup>15</sup> was proposed by Jesson and Muettterties in 1971. The mechanism consists of a shift of a hydride nucleus from an occupied to a vacant face by traversing a tetrahedral edge. This mechanism is illustrated in Scheme 2. There are, of course several other topological possibilities for the process illustrated at the top of the scheme; however, for the molecules considered in this study, there is only one unique transition state, given by **6**, for this reaction. An alternative mechanism, the double tetrahedral jump, is illustrated at the bottom of Scheme 2. It consists of simultaneous movements of both hydrogens from face positions to trans edge positions to give a trans intermediate, which is presumed to be a short-lived.

Another process proposed previously is the Ray–Dutt<sup>42</sup> mechanism. There are four possibilities for  $\text{H}_2\text{ML}_4$  rearrangement, and they are shown in Scheme 3. Here two cis ligands rotate by  $45^\circ$  and the remaining four ligands undergo a Berry pseudorotation process as illustrated by the arrows in the scheme. All four possibilities for the Ray–Dutt mechanism are illustrated. The first two processes in Scheme 3 involve the

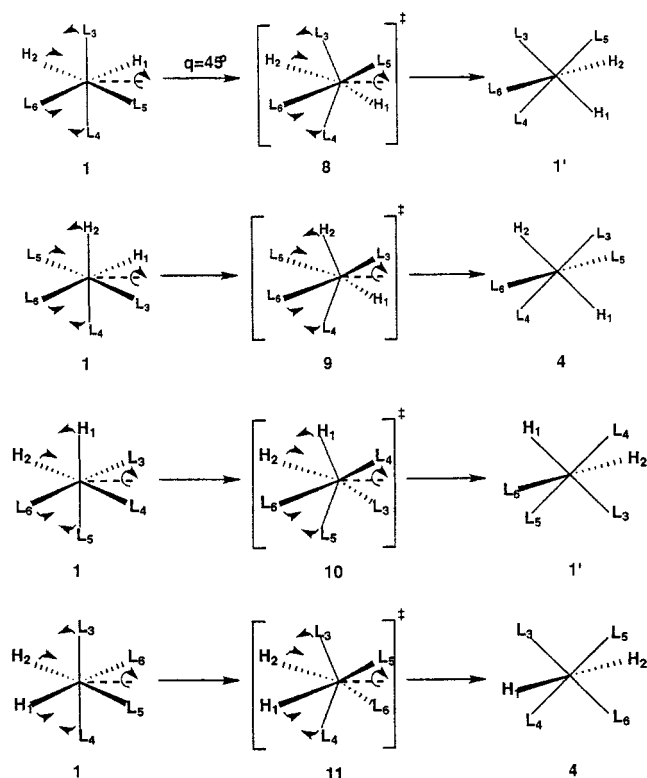
- (24) Ditchfield, R.; Hehre, W. A.; Pople, J. A. *J. Chem. Phys.* **1971**, *54*, 724.  
 (25) Hehre, W. J.; Stewart, R. F.; Pople, J. A. *J. Chem. Phys.* **1969**, *51*, 2657.  
 (26) Ehlers, A. W.; Böhme, M.; Dapprich, S.; Gobbi, A.; Höllwarth, A.; Jonas, V.; Köhler, K. F.; Stegmann, R.; Veldkamp, A.; Frenking, G. *Chem. Phys. Lett.* **1993**, *208*, 111.  
 (27) Krishnan, R.; Binkley, J. S.; Seeger, R.; Pople, J. A. *J. Chem. Phys.* **1980**, *72*, 650.  
 (28) Huzinaga, S.; Andzelm, J.; Klobukowski, M.; Radzio-Andzelm, E.; Sakai, Y.; Tawawaki, H. *Gaussian Basis Sets for Molecular Calculations*; Elsevier: Amsterdam, 1984.  
 (29) Rappe, A. K.; Smedley, T. A.; Goddard, W. A., III. *J. Phys. Chem.* **1981**, *85*, 2607. Pietro, W. J.; Hehre, W. J. *J. Comput. Chem.* **1983**, *4*, 241.  
 (30) Binkley, J. S.; Pople, J. A.; Hehre, W. J. *J. Am. Chem. Soc.* **1980**, *102*, 939.  
 (31) Möller, C.; Plesset, M. S. *Phys. Rev.* **1934**, *46*, 618.  
 (32) Krishnan, R.; Frisch, M. J.; Pople, J. A. *J. Chem. Phys.* **1980**, *72*, 4244.  
 (33) Pople, J. A.; Head-Gordon, M.; Raghavachari, K. *J. Chem. Phys.* **1987**, *87*, 5968.  
 (34) Pople, J. A.; Krishnan, R.; Schlegel, H. B.; Binkley, J. S. *Int. J. Quantum Chem.* **1978**, *14*, 545.  
 (35) Raghavachari, K. *J. Chem. Phys.* **1985**, *82*, 4607.  
 (36) Becke, A. D. *J. Chem. Phys.* **1993**, *98*, 5648.  
 (37) Becke, A. D. *Phys. Rev. A* **1988**, *38*, 3098.

- (38) Lee, C.; Yang, W.; Parr, R. G. *Phys. Rev. B* **1988**, *37*, 785.  
 (39) Vosko, S. H.; Wilk, V.; Nusair, M. *Can. J. Phys.* **1980**, *58*, 1200.  
 (40) Stevens, P. J.; Devlin, F. J.; Chablowski, C. F.; Frisch, M. J. *J. Phys. Chem.* **1994**, *98*, 11623.  
 (41) Maitre, P.; Bauschliecher, C. W., Jr. *J. Phys. Chem.* **1995**, *99*, 6836.  
 (42) Ray, P.; Dutt, N. K. *J. Indian Chem. Soc.* **1943**, *20*, 81.

## Scheme 2



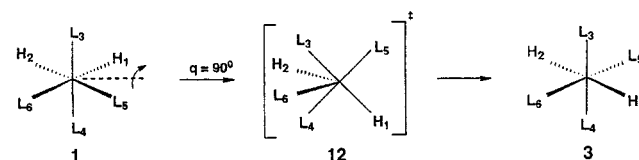
## Scheme 3



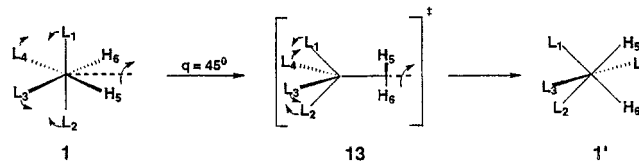
rotation of one M–H and one M–L bond by  $45^\circ$ . The difference between these two pathways is the position of the second hydrogen,  $H_2$ . In the first path,  $H_2$  occupies an equatorial cis position relative to  $H_1$ ; and in the second path, hydrogen  $H_2$  occupies an axial position, cis to  $H_1$ . In the last two mechanisms of Scheme 3, two phosphorus or carbonyl ligands are involved in a  $45^\circ$  rotation and the other two phosphorus or carbonyl ligands along with the hydrogen ligands undergo the Berry pseudorotation process. The first of these possibilities is a cis–cis isomerization proceeding via transition state **10**. The latter is a cis–trans isomerization passing through transition state **11**. The difference between these two paths again lies in the geometric positing of the two hydrides.

Burdett along with Hoffmann and co-workers proposed a bicapped tetrahedral<sup>43,44</sup> mechanism in 1976. In this reaction path, a bicapped tetrahedron transition state is produced by a

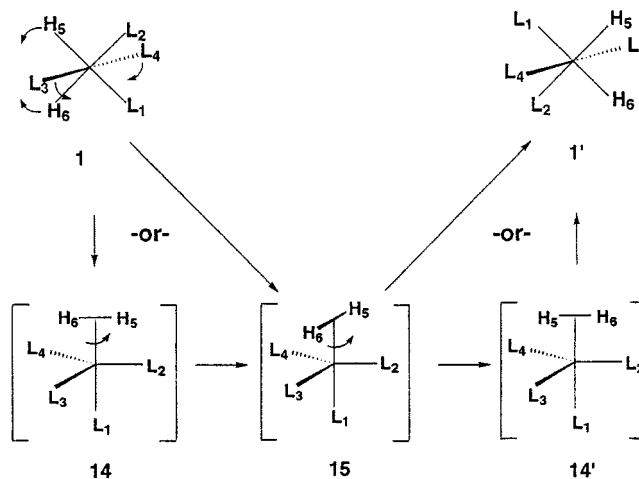
## Scheme 4



## Scheme 5



## Scheme 6



$90^\circ$  rotation of two cis ligands and an angular relaxation of the remaining ligands. This is illustrated for one example in Scheme 4. The bicapped tetrahedral mechanism shown is a cis–trans isomerization occurring via transition state **12**. Here again, there are other obvious stereochemical possibilities that involve the rotation of both hydrides or two ligands.

The ability of a transition metal dihydride to rearrange to a dihydrogen complex<sup>45</sup> suggests an alternative to the Ray–Dutt mechanism that involves a simultaneous exchange of two axial phosphorus or carbonyl ligands with the two equatorial phosphorus or carbonyl ligands. The hydride ligands simply move to the new equatorial positions as shown in Scheme 5. What distinguishes this process from the Ray–Dutt mechanism is the formation of a dihydrogen ligand in the transition state. Thus, transition state **13** can be regarded as another example of those illustrated in Scheme 3 when allowance is made for a variable H–H distance.

Given that structure **13** contains an  $\eta^2$ - $H_2$  ligand in a square pyramidal coordination environment, an alternative proposal might place this ligand in the axial position of a trigonal bipyramid. It is somewhat difficult to see how such a species could form. Starting with the cis octahedral structure, **1**, in Scheme 6, the two hydrogens couple to form a bound  $H_2$  unit which moves to the axial position. The axial phosphorus or carbon atoms narrow their angle and move to equatorial positions, while the other phosphorus or carbon atoms undergo

(43) Burdett, J. K. *Inorg. Chem.* **1976**, *15*, 212.(44) Hoffmann, R.; Howell, J. M.; Rossi, A. R. *J. Am. Chem. Soc.* **1976**, *98*, 2484.(45) For reviews, see: Heinekey, D. M.; Oldham, W. J., Jr. *Chem. Rev.* **1993**, *93*, 913. Jessop, P. G.; Morris, R. H. *Coord. Chem. Rev.* **1992**, *121*, 155. Lin, Z.; Hall, M. B. *Coord. Chem. Rev.* **1994**, *135/136*, 845. Crabtree, R. H. *Acc. Chem. Res.* **1990**, *23*, 95.

**Table 1.** Relative Energies (kcal/mol) for the Structures of H<sub>2</sub>Ru(PH<sub>3</sub>)<sub>4</sub> Optimized by Using Basis I

compd	MP2//MP2	MP4SDQ//MP2	QCISD//MP2	QCISD(T)//MP2	B3LYP//B3LYP <sup>a</sup>
<b>1</b>	0.0	0.0	0.0	0.0	0.0
<b>2</b>	36.6	37.1	41.5	42.5	
<b>4</b>	18.6	15.6	10.5	10.5	
<b>5<sup>b</sup></b>	44.1	42.4	43.1	44.0	
<b>11</b>	31.3	30.4	29.8	29.3	
<b>13</b>	51.6	46.5	51.7	53.1	42.3
<b>14</b>	24.4	22.2	24.6	25.9	
<b>15</b>	23.6	22.8	27.9	28.2	22.5

<sup>a</sup> Using basis II. <sup>b</sup> HF optimized.

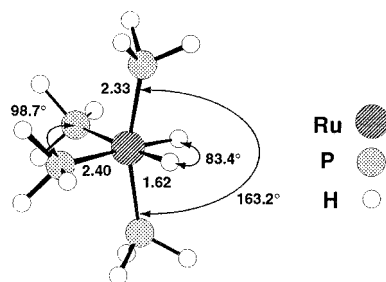


**Figure 1.** Selected geometric details for the optimized ground-state structure of H<sub>2</sub>Ru(PH<sub>3</sub>)<sub>4</sub>, **1**. The values shown were obtained at the B3LYP level.

relaxation. This forms **14** or the alternative rotomer **15**. There are then two possibilities for this type of mechanism. Either the H<sub>2</sub> ligand rotates as the ligand set in **1** undergoes the geometric motions shown in Scheme 6 to form **15** as a transition state or a structure like **14** serves as a transition state and **15** is an intermediate.

## Results

We have optimized the geometries for the structures of H<sub>2</sub>Ru(PH<sub>3</sub>)<sub>4</sub> using second-order Møller–Plesset perturbation theory (MP2). Single-point computations employing basis I have also been performed by adopting other electron correlation techniques, and the results are summarized in Table 1. Throughout this work, all four phosphine ligands were oriented in a manner that satisfies C<sub>s</sub> symmetry requirements for each structure.

Octahedral or near-octahedral geometry is overwhelmingly prevalent for six-coordinate complexes.<sup>44,46,47</sup> Selected geometric details of the B3LYP optimized structure are displayed on the left side of Figure 1. The axial PH<sub>3</sub> ligand bends toward the hydrogens forming an angle of 163.2°, and the equatorial PH<sub>3</sub> ligands widen their angle to 98.7°. This distortion from octahedral toward bicapped tetrahedral geometry has been attributed to electronic effects.<sup>44</sup> The trans influence<sup>48,49</sup> of the hydrogen ligands explains why the Ru–P<sub>eq</sub> distance is larger than the Ru–P<sub>ax</sub> distance. The geometric parameters found at the MP2 level are very close to those obtained with the B3LYP procedure. No H<sub>2</sub>Ru(PR<sub>3</sub>)<sub>4</sub> complexes have been structurally categorized. The structure of H<sub>2</sub>Ru(CO)<sub>4</sub> has been determined by microwave rotational spectroscopy.<sup>50a</sup> The Ru–H distance of 1.710(23) Å is considerably longer than our computed value of 1.62 Å. However, X-ray values of 1.630 and 1.602 Å have

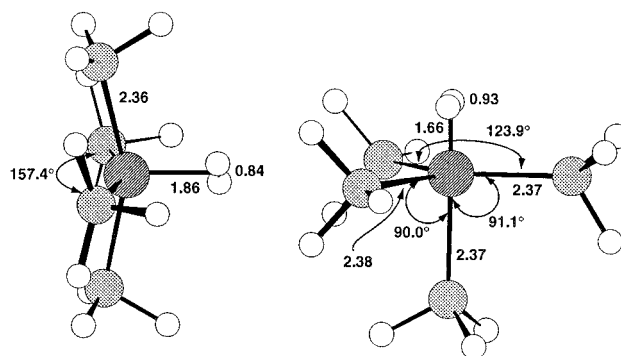


**Figure 2.** Selected geometric details for the optimized structures of the H<sub>2</sub>Ru(PH<sub>3</sub>)<sub>4</sub> isomers **13** (left) and **15** (right). The values shown were obtained at the B3LYP level.

been reported<sup>50b</sup> for two related complexes and an estimate of 1.593 Å has been made,<sup>50c</sup> all of which are more in agreement with our calculated values. The trans isomer **3** adopts an idealized octahedral geometry. The axial hydrogen ligands are separated by an angle of 180.0°, and the equatorial phosphorus ligands lie in a plane perpendicular to the H–Ru–H axis, with an angle of 90.0° between them. The cis isomer **1** is 12–19 kcal/mol more stable than the trans isomer at all levels of theory.

In an examination of the trigonal twist mechanism (Scheme 1), two stationary points, corresponding to structures **2** and **5**, were located and found to lie at high relative energies. Structure **2** is at an energy of about 37–43 kcal/mol relative to the *cis*-H<sub>2</sub>Ru(PH<sub>3</sub>)<sub>4</sub> ground state, **1**. The energy associated with **5** is even higher; it was found to be greater than 44 kcal/mol above the energy for **1** and consequently was only optimized at the HF level of theory. Special care was taken to locate a transition state associated with the single or double tetrahedral jump (Scheme 2), which was the mechanism favored by Muetterties and co-workers.<sup>1,4,5,14,15</sup> Unfortunately no stationary point corresponding to either mechanism was located. All attempts at a guess for the structures led upon optimization to the *cis* or *trans* minima. For the Ray–Dutt mechanism (Scheme 3), optimization of a structure associated with **8** gave ultimately structure **2**. A stationary point was identified with structure **11**; its relative energy was found to be about 30 kcal/mol above that of **1**. No stationary points were located for the other two structures nor were any found for the processes corresponding to Scheme 4. The Ray–Dutt mechanism involves rotation of the two hydrides by 45°. When we attempted to find a transition state associated with rotation of the two Ru–H bonds, a stationary point, **13** (see Scheme 5), was located. In other words, upon rotation, an H–H bond is formed. Selected geometric details at the B3LYP level for this structure are presented in Figure 2. The MP2 optimized values are very close to the values shown in this figure. The calculated H–H distances of 0.84 Å (or 0.83 Å at the MP2 level) are unexceptional compared to those of the experimental structures of other η<sup>2</sup>-H<sub>2</sub> complexes.<sup>45</sup> However,

(46) Dixon, D. T.; Kola, J. C.; Howell, J. A. S. *J. Chem. Soc., Dalton Trans.* **1984**, 1307.

(47) Muetterties, E. L. *J. Am. Chem. Soc.* **1968**, *90*, 5097.

(48) Burdett, J. K.; Albright, T. A. *Inorg. Chem.* **1979**, *18*, 2112.

(49) Kaesz, H. D.; Saillant, R. B. *Chem. Rev.* **1972**, *72*, 247.

(50) (a) Lavaty, T. G.; Wikrent, P.; Drouin, B. J.; Kukolich, S. G. *J. Chem. Phys.* **1998**, *109*, 9473. (b) Brammer, L.; Klooster, W. T.; Lemke, F. R. *Organometallics* **1996**, *15*, 1721. (c) Desrosiers, P. J.; Cai, L.; Lin, Z.; Richards, R.; Halpern, J. *J. Am. Chem. Soc.* **1991**, *113*, 4173.

**Table 2.** Relative Energies (kcal/mol) of the Stationary Points Located for  $\text{H}_2\text{Fe}(\text{CO})_4$  by Using Basis III

compd	HF//HF	MP2//HF	CCD//HF	ST4CCD//HF
<b>1</b>	0.0	0.0	0.0	0.0
<b>2</b>	39.1	56.2	48.6	52.3
<b>4</b>	6.9	36.3	24.8	32.9
<b>5</b>	59.2	15.7	32.1	34.5
<b>9</b>	44.9	99.5	78.8	92.3
<b>11</b>	52.5	100.3	81.2	90.0
<b>13</b>	40.4	-25.8	9.6	0.2

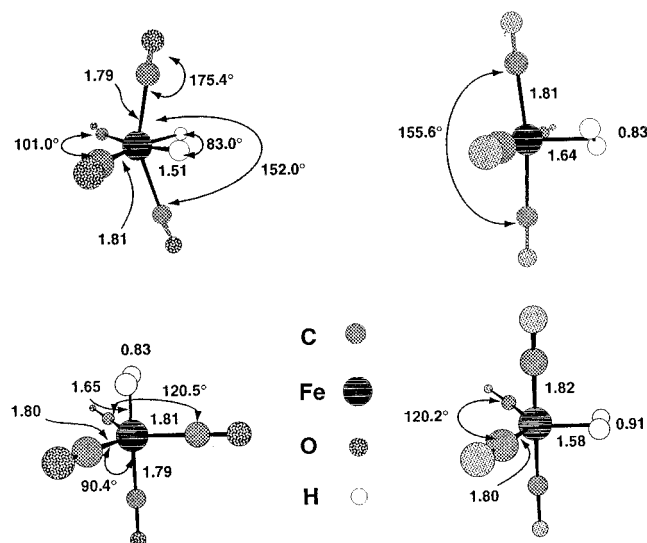
these distances are somewhat short compared to those of other  $\text{Ru}(\eta^2\text{-H}_2)$  complexes. In  $(\text{C}_5\text{Me}_5)\text{Ru}(\eta^2\text{-H}_2)(\text{dppm})^+$ ,<sup>51</sup>  $\text{Ru}(\eta^2\text{-H}_2)(\text{H})(\text{I})(\text{PCy}_3)_2$ ,<sup>52</sup> and  $\text{CpRu}(\eta^2\text{-H}_2)(\text{CO})(\text{PCy}_3)$ ,<sup>53</sup> the H–H distances were found to be 1.10(3), 1.03(7), and 0.97 Å, respectively. The Ru–H distances, computed to be 1.88 and 1.86 Å at the two levels of theory, are considerably longer than either an Ru–hydride distance or an Ru–H distance involving an  $\eta^2\text{-H}_2$  ligand, for example, 1.66(2) Å found for  $(\text{C}_5\text{Me}_5)\text{Ru}(\eta^2\text{-H}_2)(\text{dppm})^+$ <sup>51</sup> or 1.62 Å found for **1**. These structural features are consistent with an  $\text{H}_2$  complex that is undergoing a considerable amount of dissociation from the metal. Accordingly, the energy relative to that of the ground state for this structure is very high, from 42 to 53 kcal/mol, depending upon the level of theory used. On the other hand,  $\eta^2\text{-H}_2$  complexes at a much lower relative energy were located when the reaction mechanism in Scheme 6 was investigated. Structures **14** and **15** were computed to be very close in energy. However, except at the HF level, **14** was consistently found to lie at an energy lower than that of **15** (see Table 1); hence, we identified **15** as being the transition state for the process given in Scheme 6. It is computed to lie from 22 to 28 kcal/mol above the ground-state structure, depending upon the level of theory used. This is in reasonable agreement with the 18.3 kcal/mol barrier determined for  $\text{RuH}_2(\text{CO})(\text{PPh}_3)_3$ .<sup>19</sup> There is a significant difference here between the MP2 and B3LYP optimized structures. In the former, the H–H distance was computed to be 1.58 Å, which is quite long compared to those of other  $\eta^2\text{-H}_2$  structures.<sup>45</sup> At the B3LYP level, the H–H distance is predicted to be a more “normal” 0.93 Å, and we suspect that this is a more reasonable estimate. The Ru–P distance is also somewhat sensitive to the identity of the ligand trans to it. When it is a dihydride species at the MP2 level, the Ru–P distance is 0.10 Å longer than it is when the ligand is  $\text{H}_2$  at the B3LYP level. This is consistent with a hydride ligand exerting a larger trans influence compared to that of an  $\text{H}_2$  ligand.

The potential energy surface for  $\text{H}_2\text{Fe}(\text{CO})_4$  is very similar to that for its  $\text{H}_2\text{Ru}(\text{PH}_3)_4$  counterpart with few exceptions. Table 2 presents the relative energies for optimizations at the Hartree–Fock level. The same stationary points were located, with the exception that one more stationary point associated with the Ray–Dutt mechanism, **9** in Scheme 3, was located. In particular, no transition states corresponding to either of the tetrahedral jump processes (Scheme 2) were located, although numerous attempts were made. The energy of the trans isomer (structure **4**) is predicted to lie at a prohibitively high energy, from 25 to 36 kcal/mol above the energy of the cis ground state structure, which also certainly makes the double tetrahedral jump implausible. Disregarding **13** for the moment, the relative energies computed for all other structures are reasonably close to one

**Table 3.** Energies (kcal/mol) of the  $\eta^2\text{-H}_2$  Species Relative to the Ground State, **1**, Obtained by Using Basis III

method	<b>13</b>	<b>15</b>	method	<b>13</b>	<b>15</b>
HF	40.4	30.8	CISD	30.7	0.0
MP2	-25.8	-82.8	CCSD	33.0	6.1
MP4(SDQ)	-43.0	-101.0	B3LYP (IV) <sup>a</sup>	12.8	12.3
CCD	9.6	-19.2	B3LYP (V) <sup>b</sup>	13.3	13.0
ST4CCD	0.2	-28.0			

<sup>a</sup> Using basis set IV. <sup>b</sup> Using basis set V.

**Figure 3.** Selected geometric details for the optimized structures of the  $\text{H}_2\text{Fe}(\text{CO})_4$  isomers **1** (upper left), **13** (upper right), **15** (lower left) and **16** (lower right). The values shown were obtained at the B3LYP level.

another at the correlated levels. Furthermore, these energies are all very high. Whitmire and Lee have measured the barrier for axial–equatorial CO exchange by using  $^{13}\text{C}$  NMR spectroscopy.<sup>54</sup> This exchange is directly related to the mechanisms considered here. The activation energy was found to be 8.1 kcal/mol.<sup>54</sup> The CCD energy for the  $\eta^2\text{-H}_2$  transition state in **13** is very close to the experimental estimate; however, this is probably fortuitous, as shown below. A serious problem was uncovered in the description of the  $\eta^2\text{-H}_2$  species, **13** and **15**. Frequency calculations on **13** and **15** at the B3LYP level using basis IV along with HF using basis III revealed the existence of one imaginary frequency associated with each structure, thus confirming their identities as true transition states. The energies relative to the ground state structure are listed in Table 3 for a number of theoretical techniques. What is clear is that the only method with some consistency is the hybrid density functional B3LYP. The Møller–Plesset perturbation series does not converge, given the very serious errors associated with the relative energies of **13** and **15** at the MP4(SDQ) level (a negative value means that the structure is calculated to be more stable than the ground-state minimum). While CCD theory is close to experiment for **13**, it is in gross error for **15**, and so on. We shall discuss this situation further in the next section.

The structural parameters for several stationary points in  $\text{H}_2\text{-Fe}(\text{CO})_4$  are shown in Figure 3. The numbers are taken from the B3LYP optimizations. The optimized structure for the ground state, **1**, at the top left of Figure 3 is very close to experiment.<sup>55</sup> This was previously established by Drouin and Kukulich,<sup>55b</sup> who used a slightly different basis set and density functional. On the other hand, the Fe–H and Fe–C distances

(51) Klooster, W. T.; Koetzle, T. F.; Jia, G.; Fong, T. P.; Morris, R. H.; Albinati, A. *J. Am. Chem. Soc.* **1994**, *116*, 7677.

(52) Chaudret, B.; Chung, G.; Eisenstein, O.; Jackson, S. A.; Lahoz, F. J.; Lopez, J. A. *J. Am. Chem. Soc.* **1991**, *113*, 2314.

(53) Zilm, K. W.; Millar, J. M. *Adv. Magn. Opt. Reson.* **1990**, *15*, 163.

(54) Whitmire, K. H.; Lee, T. R. *J. Organomet. Chem.* **1985**, *282*, 95.

are uniformly too long at the HF level. Furthermore, the HF method predicts the Fe–C–O angles to be somewhat less than 180° when in fact they are not<sup>55</sup> nor is this feature found in the isoelectronic H<sub>2</sub>Ru(CO)<sub>4</sub><sup>50a</sup> and H<sub>2</sub>Os(CO)<sub>4</sub><sup>56</sup> molecules. The other structural features, including the deformation toward a bicapped tetrahedron, are close to experiment for both methods. The two structures which correspond to the two transition states **13** and **15** at the upper right and lower left, respectively, in Figure 3, also display similar characteristics although, in this case, the Fe–C–O angles are computed (at the HF level) to be close to linear. The HF optimized geometries yield  $\eta^2$ -H<sub>2</sub> structures that are less strongly bound to the metal than those at the B3LYP level, as judged by longer Fe–H and shorter H–H distances.

What is most unusual was the location of another minimum on the potential energy surface by using the B3LYP method. This structure, **16**, is shown on the lower right of Figure 3. Using the smaller basis set IV, frequency calculations reveal that it is a minimum. It is found to lie 10.0 and 9.1 kcal/mol above the ground state using basis IV and basis V, respectively. This same result is obtained with the HFB and B3P86 DFT methods. With basis IV, HFB and B3P86 predict that the energy of **16** is 9.0 and 11.3 kcal/mol, respectively, above the energy of **1**. Furthermore, a frequency calculation using B3P86 also reveals that **16** is a local minimum. Therefore, the type of functional used does not appear to influence the existence of this structure. No stationary point analogous to **16** was located with the HF method. On the other hand, an MP2 optimization starting from a geometry close to the experimental ground state, yielded only one structure, which geometrically was very similar to **16**. In other words, no dihydride structure corresponding to **1** was located. The same result was also obtained recently by Jonas and Thiel.<sup>57</sup> The ramifications of **16** will be more fully discussed in the next section.

## Discussion

For both H<sub>2</sub>Fe(CO)<sub>4</sub> and H<sub>2</sub>Ru(PH<sub>3</sub>)<sub>4</sub>, only  $\eta^2$ -H<sub>2</sub> structures were found as viable transition states for these polytopal rearrangements. The activation energies for rearrangements involving a trigonal twist or other related processes were computed to be far too high at all levels of theory, or we were unable to locate the transition states (particularly in the case of the tetrahedral jump mechanisms) that have been proposed by others.<sup>1,5,14,15,19</sup> An  $\eta^2$ -H<sub>2</sub> species was proposed by Berke and co-workers<sup>58</sup> as a transition state for the polytopal rearrangements of H<sub>2</sub>Re(CO)(NO)(PR<sub>3</sub>). Their proposal involved the formation of an  $\eta^2$ -H<sub>2</sub> ligand at the equatorial position of a trigonal bipyramidal complex which then underwent a rigid rotation about the metal–H<sub>2</sub> axis. For electronic reasons, we do not believe that this is the case. The H<sub>2</sub> ligand has valence orbitals,  $\sigma$  and  $\sigma^*$ , which are topologically analogous to the  $\pi$  and  $\pi^*$  orbitals of ethylene. Thus, the bonding in ( $\eta^2$ -H<sub>2</sub>)Fe(CO)<sub>4</sub> is isolobal with that in ( $\eta^2$ -ethylene)Fe(CO)<sub>4</sub>. In ( $\eta^2$ -ethylene)Fe(CO)<sub>4</sub>, it has been shown<sup>59,60</sup> that rotation about the

olefin–Fe bond is accompanied by pseudorotation of the Fe(CO)<sub>4</sub> unit. We find this also to be true here, so that the mechanism (Scheme 5) is one where H–H coupling is accompanied by rotation about the Fe–H<sub>2</sub> axis along with pseudorotation. The transition state is then a square pyramid with the H<sub>2</sub> unit rotated by 45° rather than a trigonal bipyramid where the H<sub>2</sub> unit is rotated by 90°.<sup>58</sup>

What is perhaps perplexing, at first sight, is that the transition state for this pseudorotation–rotation process, **13**, lies at a very high relative energy for H<sub>2</sub>Ru(PH<sub>3</sub>)<sub>4</sub>. This is the case (Table 1) for all of the theoretical techniques used in our study. However, our calculations clearly point to **15** with its attendant more difficult motion as being the transition state. There is actually good experimental precedent for **15**, and in fact, an analogous structure has been proposed by Heinekey and co-workers<sup>61</sup> for the polytopal rearrangements observed in H<sub>2</sub>M[P(CH<sub>2</sub>CH<sub>2</sub>-PPh<sub>2</sub>)<sub>3</sub>]<sup>+</sup> where M = Co, Rh, and Ir. While the tetradentate ligand in this complex is not typical and certainly favors the formation of a structure like **15**,<sup>61</sup> we nevertheless feel that there is a good electronic rationale for why **15** is preferred over **13** for the Ru complex and we suspect any other case where M is a second or third transition metal and L is a strong  $\sigma$ -donor. If we put aside, for a moment, the obvious theoretical problems associated with the relative energies in H<sub>2</sub>Fe(CO)<sub>4</sub>, the most likely situation is that the B3LYP values are the reasonable ones, and here the relative energies of **13** and **15** are quite close. We think that all of these findings can be rationalized in the following way: An orbital interaction diagram for a d<sup>8</sup> ( $\eta^2$ -H<sub>2</sub>)-ML<sub>4</sub> complex at structure **13** is presented in Figure 4. On the left side are the important valence orbitals of a square pyramidal ML<sub>4</sub> fragment.<sup>60</sup> Four d orbitals, 1a<sub>1</sub>, 1b<sub>1</sub>, 1b<sub>2</sub>, and 2a<sub>1</sub>, lie at low to moderate energies. The fifth d orbital is much higher in energy and is not shown in the figure. The H<sub>2</sub>  $\sigma$  orbital overlaps with the 2a<sub>1</sub> and 3a<sub>1</sub> orbitals on the ML<sub>4</sub> fragment. Of the three molecular orbitals that are created, the lowest bonding and middle nonbonding MOs are occupied. What is critical in this analysis is the back-bonding from the 1b<sub>2</sub> orbital on ML<sub>4</sub> to the H<sub>2</sub>  $\sigma^*$  orbital. When the 1b<sub>2</sub> orbital lies high in energy and overlaps well with the  $\sigma^*$  orbital, a strong interaction is created. Much electron density flows from the 1b<sub>2</sub> orbital to the  $\sigma^*$  orbital, and, therefore, the H–H bond is severely weakened. It would be energetically advantageous to relax this geometry to one with a long H–H bond length. In other words, if this interaction is strong, then the energy required to attain an  $\eta^2$ -H<sub>2</sub> structure is expected to be large and the H<sub>2</sub> unit will need to be significantly dissociated from the ML<sub>4</sub> group. This is precisely the case for the H<sub>2</sub>Ru(PH<sub>3</sub>)<sub>4</sub> complex. Recall from Figure 1 that the H–H distance is quite short and the Ru–H distance is long for **13**. On the other hand, in H<sub>2</sub>Fe(CO)<sub>4</sub>, the  $\sigma$ -donor phosphine ligands have been replaced by  $\pi$ -acceptor carbonyls. Consequently, the 1b<sub>2</sub> orbital of the Fe(CO)<sub>4</sub> fragment is expected to lie lower in energy than that of Ru(PH<sub>3</sub>)<sub>4</sub> and back-bonding will then not be as strong. Likewise, a 3d AO is much more contracted and overlaps with the H<sub>2</sub>  $\sigma^*$  orbital less than does a 4d AO. Hence, on the basis of energy gap and overlap considerations, back-bonding from the Fe(CO)<sub>4</sub> fragment is weaker, so the energy required to attain structure **13** is smaller than that for a Ru(PH<sub>3</sub>)<sub>4</sub> fragment. The bonding situation for a molecule in geometry **15** is quite similar. An orbital interaction diagram is displayed in Figure 5. Here, all five d orbitals lie at low to moderate energies. The 3a' fragment orbital

(55) (a) McNeil, E. A.; Scholer, F. R. *J. Am. Chem. Soc.* **1977**, *99*, 6243.

(b) Drouin, B. J.; Kukulich, S. G. *J. Am. Chem. Soc.* **1998**, *120*, 6774.

(56) Kukulich, S. G.; Sickafoose, S. M.; Breckenridge, S. M. *J. Am. Chem. Soc.* **1996**, *118*, 205.

(57) Jonas, V.; Thiel, W. *J. Chem. Phys.* **1996**, *105*, 3636.

(58) Bakhmutov, V.; Bürgi, T.; Burger, P.; Ruppli, U.; Berke, H. *Organometallics* **1994**, *13*, 4203.

(59) Albright, T. A.; Hoffmann, R.; Thibault, J. C.; Thorn, D. L. *J. Am. Chem. Soc.* **1979**, *101*, 3801.

(60) Albright, T. A.; Burdett, J. K.; Whangbo, M.-H. *Orbital Interactions in Chemistry*; Wiley: New York, 1985.

(61) Heinekey, D. M.; Liegeois, A.; van Roon, M. *J. Am. Chem. Soc.* **1994**, *116*, 8388. Heinekey, D. M.; van Roon, M. *J. Am. Chem. Soc.* **1996**, *118*, 12134.

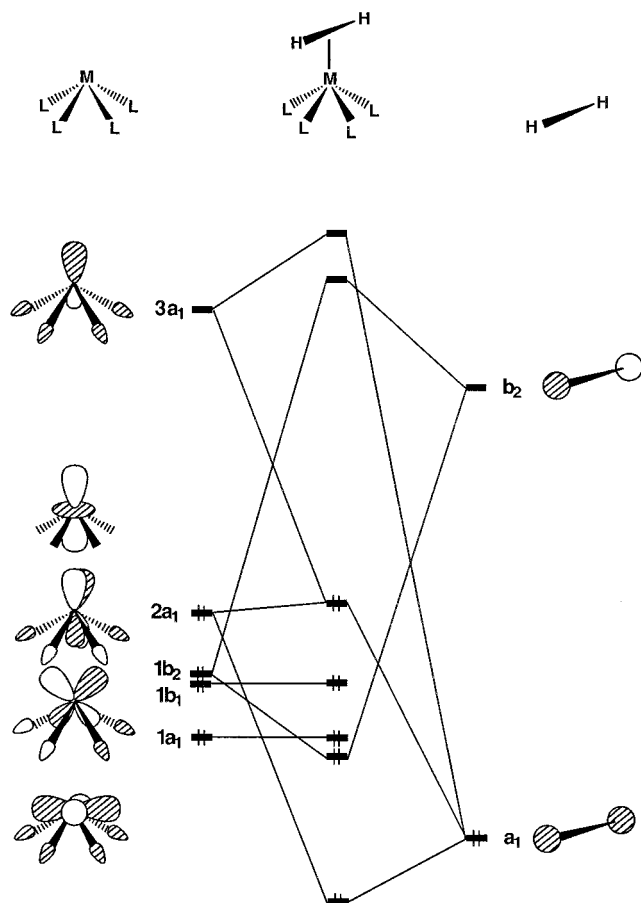


**Figure 4.** Orbital interaction diagram for the construction of the important valence orbitals in a  $d^8$  ( $\eta^2$ -H<sub>2</sub>)ML<sub>4</sub> at structure **13**.

of ML<sub>4</sub> interacts with and stabilizes the H<sub>2</sub>  $\sigma$  orbital. This is very similar to the role of the 3a<sub>1</sub>–H<sub>2</sub>  $\sigma$  interaction in Figure 4. Back-donation to the H<sub>2</sub>  $\sigma^*$  orbital now occurs via the 1a'' fragment orbital, which lies at lower energy than the 1b<sub>2</sub> counterpart in Figure 4, since the latter fragment orbital is somewhat M–L antibonding whereas the 1a'' orbital is truly transition metal nonbonding to a ligand  $\sigma$ -donor function. Therefore, particularly for the H<sub>2</sub>Ru(PH<sub>3</sub>)<sub>4</sub> molecule, a structure akin to **15**, where back-bonding, is smaller is more easily attained.

A number of studies<sup>62</sup> have pointed out difficulties with attaining reliable results for molecules that, in particular, possess a metal atom from the first transition metal row. This problem is still being investigated, but the center of attention has focused on the fact that the small radial extent of the 3d AOs creates severe correlation problems. The commonly used Møller–Plesset perturbation techniques succeed sometimes, but are divergent other times, as they are in this case (see Table 3). An interesting thesis has been advanced<sup>62</sup> that the problem is one of dynamic correlation where it is necessary to take single excitations into account. But note from Table 3 that the ST4CCD and CISD treatments clearly result in gross errors. Given our arguments that the stabilities of **13** and **15** should be roughly comparable, the CCSD method puts **13** at a much too high energy. Other studies<sup>62</sup> which have included very problematic cases from the first transition metal row have found the CCSD technique to perform admirably. One can see in Table 3 that

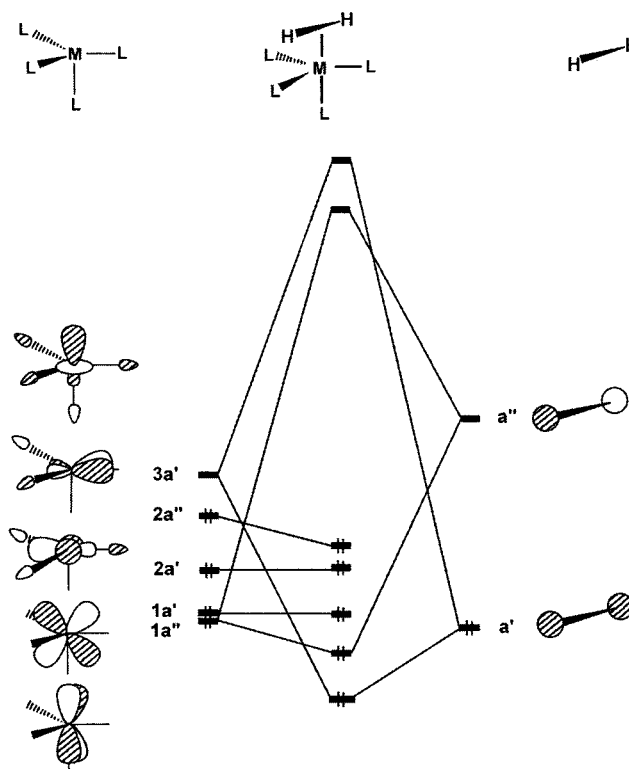


**Figure 5.** Orbital interaction diagram for a  $d^8$  ( $\eta^2$ -H<sub>2</sub>)ML<sub>4</sub> molecule at geometry **15**.

the relative energy difference between **13** and **15** is essentially constant at 28 kcal/mol on going from the CCD to ST4CCD to CCSD levels. In other words, the position of the ground state is being stabilized relative to the two transition states in this series. The B3LYP density functional approach, on the other hand, puts the relative energies of **13** and **15** close to each other and within the experimental estimate.<sup>54</sup> We also optimized structure **13** with a different functional, at the B3P86 level, and found it to be 14.8 kcal/mol above the ground-state structure. This is also not consistent with the CCSD results. Therefore, we feel that the DFT results putting **13** and **15** at nearly identical energies are more likely to be correct. We encourage additional research at higher levels.

Finding minimum-energy structures that correspond to a dihydride (**1**) and to an  $\eta^2$ -H<sub>2</sub> complex (**16**) where the ML<sub>4</sub> geometry is essentially unaltered at several DFT levels of theory we feel is somewhat suspect. It can readily be established that the conversion of an ( $\eta^2$ -H<sub>2</sub>)ML<sub>n</sub> species to an H<sub>2</sub>ML<sub>n</sub> species by simply stretching the H–H bond is symmetry allowed for any ML<sub>n</sub> species. It is therefore difficult to envision any circumstance where there would be a barrier that interconverts these two structures when only such a simple geometric motion is required. In fact, one can regard the conversion of **1** to **16** as being an example of bond-stretch isomerism,<sup>60</sup> except that in previously examined cases the existence of two separate potential energy wells separated by a barrier is predicated by the existence of two different electronic states for the molecule in question. This is not the case here. Attempts at the optimization of a structure analogous to **16** at the HF level resulted in collapse back to **1**. As noted in the previous section, optimization of H<sub>2</sub>Fe(CO)<sub>4</sub> at the MP2 level starting with the HF geometry produced a structure akin to **16**; no dihydride structure could be found. When H<sub>2</sub> reacts with Fe(CO)<sub>4</sub>, a van der Waals type complex undoubtedly is initially formed. This cannot correspond to **16** for two reasons. As indicated in Figure

(62) See, for example: Koch, H.; Jørgensen, P.; Helgaker, T. *J. Chem. Phys.* **1996**, *104*, 9528. Blomberg, M. R. A.; Siegbahn, P. E. M.; Svensson, M. *J. Chem. Phys.* **1996**, *104*, 9546 and references therein.

3, the structural difference between **1** and **16** lies in the widening of the equatorial C–Fe–C angle from 101.0 to 120.2° and the opening of the axial C–Fe–C angle from 152.0 to 177.9° along with, of course, a decrease in the H–H bond length from 2.00 to 0.91 Å. The important point is that the Fe–H bond length only increases by 0.07 Å on going from **1** to **16**. One would expect a much longer bond length for a van der Waals complex. In addition, the energy for the dissociation of H<sub>2</sub> from H<sub>2</sub>Fe(CO)<sub>4</sub> has been measured as being 20.5 ± 2.1 kcal/mol.<sup>63</sup> The van der Waals minimum should lie in a shallow potential energy well and, therefore, lie just below the dissociation limit, and yet its energy of 9–11 kcal/mol relative to **1** is much smaller than this. The existence of **16** was also recently found by Drouin and Kukolich,<sup>55b</sup> by Wang and Weitz,<sup>64</sup> and by Frenking and co-workers<sup>65</sup> using DFT methods. Finally, several attempts were made at finding a minimum like **16** for H<sub>2</sub>Ru(PH<sub>3</sub>)<sub>4</sub> with the B3LYP technique; however, no structure was found and all attempts led back to the ground-state structure, **1**. Macgregor and co-workers<sup>66</sup> have also used DFT calculations to probe the addition of H<sub>2</sub> to M(PH<sub>3</sub>)<sub>4</sub> where M = Ru, Rh<sup>+</sup>, and Fe. An

intermediate along the reaction pathway akin to structure **16** was not reported. Our suspicion is that the prediction of a minimum-energy species akin to **16** is an artifact of the DFT and MP2 methods. We encourage further studies in this area, and in this regard, we note that other workers,<sup>67</sup> using MP2 geometry optimizations, have predicted the existence of dihydride and  $\eta^2$ -H<sub>2</sub> structures similar to those of **1** and **16** for H<sub>2</sub>M(CO)<sub>4</sub>L complexes.

### Conclusions

We have shown that the mechanism for polytopal rearrangement in H<sub>2</sub>Ru(PH<sub>3</sub>)<sub>4</sub> occurs via a trigonal bipyramidal transition state (**15** in Scheme 6) where an  $\eta^2$ -H<sub>2</sub> ligand is coordinated to the axial position. For H<sub>2</sub>Fe(CO)<sub>4</sub>, a transition state geometrically analogous to this one and a transition state having an  $\eta^2$ -H<sub>2</sub> ligand coordinated in the apical position of a square pyramid (**13** in Scheme 5) are found to be at the lowest energies. All methods demonstrate that the other mechanisms which have been proposed are not viable ones for both compounds. While there is general agreement between the theoretical techniques for H<sub>2</sub>Ru(PH<sub>3</sub>)<sub>4</sub>, there are grave problems posed by the different methods used in this study concerning the relative energies for  $\eta^2$ -H<sub>2</sub> isomers of H<sub>2</sub>Fe(CO)<sub>4</sub>.

**Acknowledgment.** We thank the Robert A. Welch Foundation for generous support of this work.

IC0006089

(63) Wang, W.; Narducci, A. A.; House, P. G.; Weitz, E. *J. Am. Chem. Soc.* **1996**, *118*, 8654.

(64) Wang, W.; Weitz, E. *J. Phys. Chem. A* **1997**, *101*, 2358.

(65) Torrent, M.; Solà, M.; Frenking, G. *Organometallics* **1999**, *18*, 2801.

(66) Macgregor, S. A.; Eisenstein, O.; Whittlesey, M. K.; Perutz, R. N. *J. Chem. Soc., Dalton Trans.* **1998**, 291.

(67) Dapprich, S.; Frenking, G. *Organometallics* **1996**, *15*, 4547.